[Global Biogeochemical Cycles]

Supporting Information for

Dissolved, labile and total particulate trace metal dynamics on the northeast Greenland Shelf

Xue-Gang Chen[1, 2, *], Stephan Krisch[2, 3], Ali Al-Hashem[2], Mark James Hopwood[4], Michiel M. Rutgers van der Loeff [5], Oliver Huhn[6], Pablo Lodeiro[7], Tim Steffens[2], Eric P. Achterberg[2, *]

[1] Ocean College, Zhejiang University, 316021 Zhoushan, China
[2] GEOMAR Helmholtz Centre for Ocean Research Kiel, 24118 Kiel, Germany
[3] Now at Bundesanstalt für Gewässerkunde, Am Mainzer Tor 1, 56068 Koblenz
[4] Department of Ocean Science and Engineering, Southern University of Science and Technology, Shenzhen, China
[5] Alfred Wegener Institute, Helmholtz Centre for Polar and Marine Research, Bremerhaven, Germany
[6] IUP - Institute of Environmental Physics, University of Bremen, Bremen, Germany
[7] Department of Chemistry, Universitat de Lleida – AGROTECNIO-CERCA Center, Rovira Roure 191, 25198, Lleida, Spain

To whom correspondence should be addressed:
Xue-Gang Chen, xchen@geomar.de, chenxg83@zju.edu.cn
Eric P. Achterberg, eachterberg@geomar.de

Contents of this file:

Supplementary methods

Trace elements

Trace metal samples were collected using the ultra-clean CTD (ucCTD) rosette, equipped with 24 × 12 L GoFlo bottles following GEOTRACES sampling protocols (Cutter et al., 2017). Marine particle samples collected on acid pre-cleaned polyethersulfone (PES) filters (0.2 µm pore-size; 25 mm diameter, Sartorius) were processed sequentially to determine labile and refractory particulate trace elements (Cd, Co, Fe, Mn, Cu, Ni, P, Al, Ti, and V) using the methods as per Al-Hashem et al. (2022). The labile particulate fractions were determined following a chemical leach application consisting of a weak acid (25% acetic acid, Optima grade, Fisher Scientific) with a mild reducing agent (0.02 M hydroxylamine hydrochloride, Sigma trace metal grade), and included a short heating step (10 min, 90 - 95°C), with a total leach time of 2 hours (Berger et al., 2008), and was subsampled from afterwards. Residual (refractory) particles were subsequently digested following a 15 h reflux digest at 150 °C using a mixture of hydrofluoric and nitric acid (50% and 10% by volume, respectively, Optima grade, Fisher Scientific) (Cullen & Sherrell, 1999), with the sample filter adhered to the inner was of the perfluoroalkoxy (PFA) digestion vessels (Savillex).

Dissolved trace metals (dTMs, Cd, Co, Fe, Mn, Cu, and Ni) and particulate trace elements were then measured via high-resolution inductively coupled plasma-mass spectrometry (HR-ICP-MS; Thermo Fisher Element XR). Briefly, for dTMs, 15 mL sample aliquots were pre-concentrated using an automated SeaFAST system (SC-4 DX SeaFAST pico; ESI) exactly as per Rapp et al. (2017). All reagents for SeaFAST were prepared in deionized water (>18.2 MΩ cm^{-1}; Milli-Q, Millipore). A solution of 1 M single-distilled sub-boiled HNO_3 (SpA grade, Romil) was used for sample elution. Ammonium acetate buffer (pH 8.5) was prepared from glacial acetic acid and ammonium hydroxide (Optima, Fisher Scientific). Ten-fold pre-concentrated samples were then analyzed with calibration via isotope dilution for Fe, Ni, Cu, and Cd, and standard addition for Mn and Co. Labile and total particulate analyses were measured without pre-concentration and quantified using external multi-element calibration using multi-element standards (Inorganic Ventures) prepared in the same sample matrix (Cullen et al., 2001). The total

particulate trace element concentrations reported are the sum of labile and refractory particulate fractions.

The precision and accuracy of dTM measurements were reported by (Krisch et al., 2021, 2022). The validation of labile and total particulate trace metal analyses was monitored by reference materials BCR-414 and PACS-3 (Table S1).

Table S1 Procedural blanks, limits of detection, and measured and concentrations of Al, Fe, Ti, P, Mn, Cu, Ni, Co, Cd, and V for Reference materials BCR-414 and PACS-3. Detection Limits were determined as 3× the standard deviation (SD) of procedural blanks. Certified Reference Material (CRM) recoveries were determined using certified values and consensus values acquired from the GeoReM database at the time of publication (Jochum et al., 2005). *n* = number of measurements.

	n	Al	Fe	Ti	P	Mn	Cu	Ni	Co	Cd	V
Average Process Blank LpTM (ng/filter ± 1 SD)	*7*	2.60 ± 1.90	5.18 ± 0.74	0.11 ± 0.11	8.39 ± 14.0	0.15 ± 0.09	0.65 ± 0.23	0.65 ± 0.14	0.03 ± 0.01	0.011 ± 0.005	0.04 ± 0.02
LpTM Detection Limit (ng/filter)		5.70	2.23	0.32	42.06	0.28	0.70	0.43	0.03	0.013	0.05
Average Process Blank TpTM (ng/filter ± 1 SD)	*5*	11.27 ± 14.54	10.47 ± 14.31	3.68 ± 4.19	2.57 ± 2.90	0.12 ± 0.20	0.37 ± 0.37	0.07 ± 0.06	0.01 ± 0.01	0.002 ± 0.002	0.02 ± 0.03
TpTM Detection Limit (ng/filter)		43.62	42.94	12.57	8.69	0.60	1.10	0.19	0.02	0.004	0.10
BCR-414 Certified/Ref. Values (ng/mg ± 1 SD)		2673 ± 96	1850 ± 190	126 ± 4	14123 ± 852	299 ± 13	29.5 ± 1.3	18.8 ± 0.8	1.43 ± 0.06	0.383 ± 0.014	8.1 ± 0.18
BCR-414 measured values (Total, ng/mg ± 1 SD)	6	3054 ± 165	2061 ± 99	142 ± 8.7	16170 ± 2915	274 ± 13	29.7 ± 2.3	19.6 ± 2.5	1.54 ± 0.07	0.447 ± 0.058	10.1 ± 0.76
PACS-3 Certified/Ref. Values (ng/mg ± 1 SD)		65800 ± 1200	41060 ± 640	4420 ± 180	937 ± 44	432 ± 16	326 ± 10	39.5 ± 2.2	12.1	2.23 ± 0.16	129 ± 8
PACS-3 measured values (Total, ng/mg ± 1 SD)	4	55832 ± 1156	34724 ± 888	4219 ± 197	1050 ± 70	418 ± 9.3	295 ± 9.6	61.5 ± 2.1	13.4 ± 0.25	2.54 ± 0.26	141 ± 1.6

Macronutrients

Seawater samples for macronutrient analyses were also obtained from large volume CTD bottles. Unfiltered surface macronutrient samples (upper 200 m) were stored at 5°C and analyzed within 18 h at sea using a QUAATRO autoanalyzer (Grasshoff et al., 1999) modified according to methods provided by the manufacturer (Seal, Alliance). At all other depths, filtered samples (0.2 µm) were frozen and analyzed at Alfred Wegener Institute for Polar and Marine Research (AWI) using the same procedure.

Stable oxygen isotopes

Samples for noble gases (He and Ne) and $\delta^{18}O$ were derived from the large volume CTD (lvCTD) rosette. Stable oxygen isotopes ($\delta^{18}O$) were analyzed following Meyer et al. (2000). In short, seawater samples were equilibrated for 6.5 h using CO_2 gas of known isotopic composition and platinum as a catalyst. Equilibrated CO_2 gas was transferred into a Finnigan MAT Delta-S mass spectrometer equipped with two equilibration units, where $\delta^{18}O$ was analyzed a total of eight times. All $\delta^{18}O$ values are reported relative to a V-SMOW standard.

Noble gases

Helium and Ne concentrations were determined by Huhn, Rhein, & Kanzow, et al. (2021) following Sültenfuß et al. (2009). Gases trapped in copper tube samples were transferred into a glass ampoule at liquid nitrogen temperature and were then analyzed by a fully automated ultra-high vacuum mass spectrometric system equipped with a two-stage cryogenic trap system. The measurement uncertainties for He and Ne were ± 0.4%. The equilibria of He and Ne in seawater were calculated using the solubility function proposed by Weiss (1971). Helium excess (ΔHe) and Ne excess (ΔNe) were then calculated using the following equation:

$$\Delta C = 100*(C^{obs}/C^{eq}-1)\% \quad (1)$$

$$\Delta(He/Ne) = 100*([He^{obs}/Ne^{obs}]/[He^{eq}-Ne^{eq}]-1)\% \quad (2)$$

Where *C* is He or Ne, the superscripts *obs* and *eq* denotes observed and equilibrate values, respectively.

Radium isotopes

Seawater for radium isotopic analyses were filtered by 0.8 µm Supor (polyether sulfone) filters using an in-situ pump. Then radium isotopes were adsorbed onto MnO_2-

coated cartridges. For samples with depths of 10, 50, or 350 m, two cartridges were mounted to calculate the adsorption efficiency of radium isotopes. Only one cartridge was used for the samples at other depths. The MnO_2-coated cartridges were leached by Soxhlet extraction with 6 N HCl refluxing over 10 h. Radium in the extracts was subsequently co-precipitated with $BaSO_4$ as per Cutter et al. (2017). Radium isotopic activities (^{226}Ra, ^{228}Ra) were measured with gamma spectrometry using the procedures as per Rutgers van der Loeff et al. (2018).

Physical Oceanography

Full depth profiles of physical oceanographical parameters (salinity, potential temperature, pressure, light transmission, density, conductivity) and UV-light fluorescence were recorded by SEA-BIRD SBE 911 ucCTD and SEA-BIRD SBE 911 plus lvCTD rosettes at high resolution (m^{-1}).

Data acquisition and merge

The lvCTD bottle samples were simultaneously determined for $\delta^{18}O$, noble gases, and physical oceanographical parameters (Huhn, Rhein, Bulsiewicz, et al., 2021; Kanzow et al., 2017a; Meyer et al., 2021). Hence, the available data for these parameters were merged for all samples according to their bottle numbers and station labels. The data for labile and particulate trace elements, and macronutrients from the ucCTD observations were combined in the same way. Physical oceanographical parameters (e.g., potential temperature, transmission, and salinity) measured with ucCTD observations (Kanzow et al., 2017b) were matched to each sample allowing a maximum depth discrepancy of < 0.5 m (real uncertainty in the properties of sampled water is likely higher than this due to the inherent limitations of bottle flushing on the sampling rosette). If more than one physical oceanographical observation fulfilled this criterium, average values were taken.

The datasets of lvCTD and ucCTD observations were then merged for subsequent discussions. Because the positions and timing of the ucCTD and large CTD casts were slightly different even when deployed in rapid succession at the same location, we allowed a depth discrepancy of < 1 m in joining the lvCTD and ucCTD datasets (again, in reality the uncertainty in depth discrepancies between multiple casts is likely higher than this due to the inherent limitations associated with bottle closing and flushing). Four samples with a depth difference of 5 m and three bottom samples with a depth discrepancy of 7 – 20 m

were also merged by carefully comparing their physical oceanographical parameters. The almost identical physical oceanographical conditions (e.g., salinity, potential temperature, and density) between lvCTD and ucCTD observations (Fig. S1) demonstrate our data processing is reliable. For instance, most samples exhibit density differences of < 0.06 kg m^{-3} between the lvCTD and ucCTD datasets. Relatively high density and salinity discrepancies are confined to near surface samples with depths < 30 m which is expected in a strongly stratified water column. Our following discussions are not influenced by these samples because the merging of both datasets is used to discriminate the influence of freshwater exiting the 79NG cavity (the submarine meltwater), which is generally significant at depths > 50 m (Huhn, Rhein, Kanzow, et al., 2021). Any data deficiency ($\delta^{18}O$, noble gas, and radium isotope data are not available for several samples) is annotated as 'not determined'. 'Not determined' data are excluded during statistical analyses.

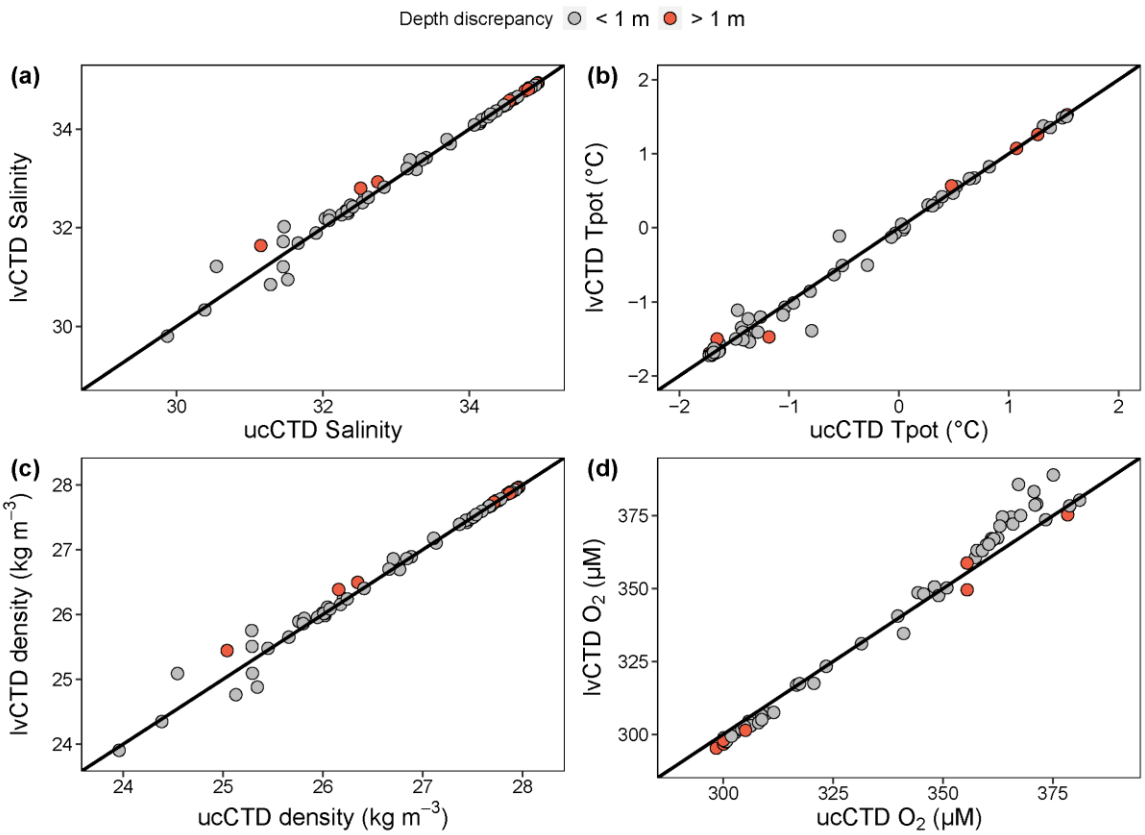

Fig. S1 Correlations between physical oceanographical parameters (salinity, density, potential temperature (Tpot), and O_2) in the combined large volume CTD (lvCTD) and ultraclean CTD (ucCTD) observations. The black lines illustrate equivalent lines. The grey and red dots indicate the depth discrepancy during joining of lvCTD and ucCTD observations.

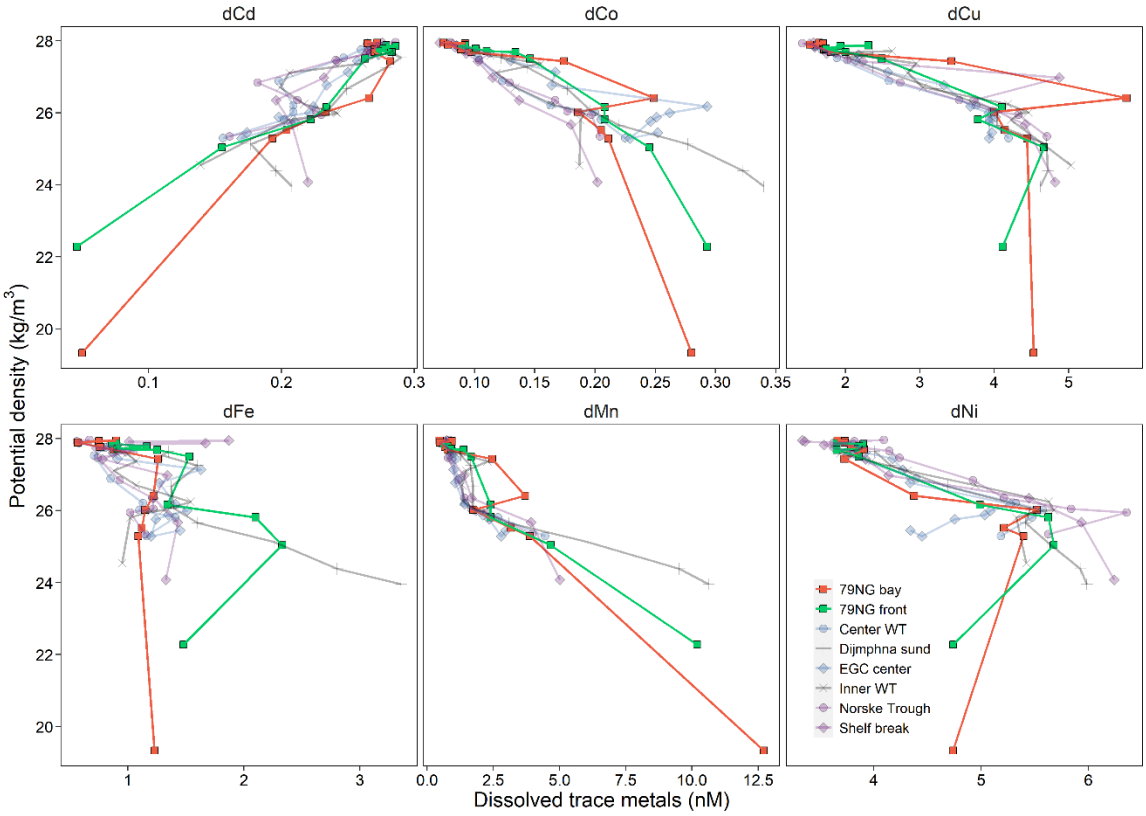

Fig. S2 Distribution profiles of dTMs (dCd, dCo, dCu, dFe, dMn, and dNi) against potential density on the NE Greenland shelf.

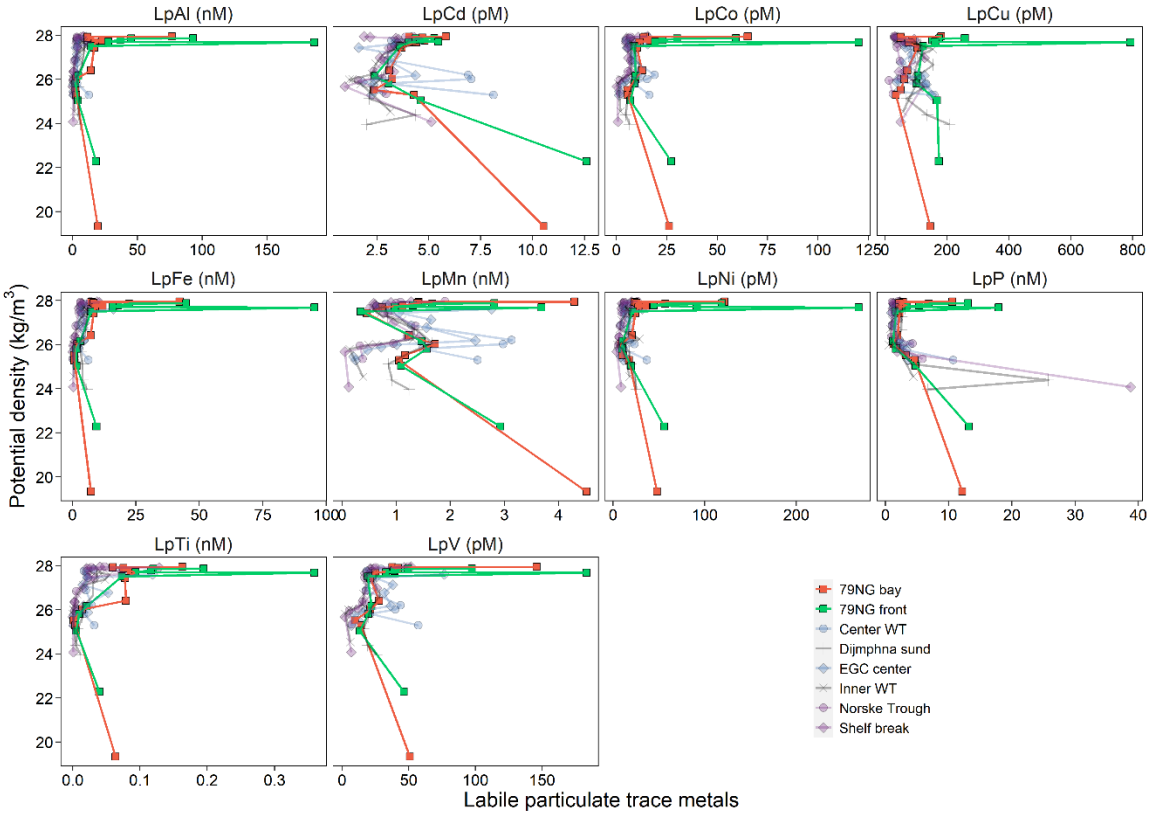

Fig. S3 Distribution profiles of labile particulate (Lp) Cd, Co, Cu, Fe, Mn, Ni, Al, Ti, V, and P against potential density on the NE Greenland shelf.

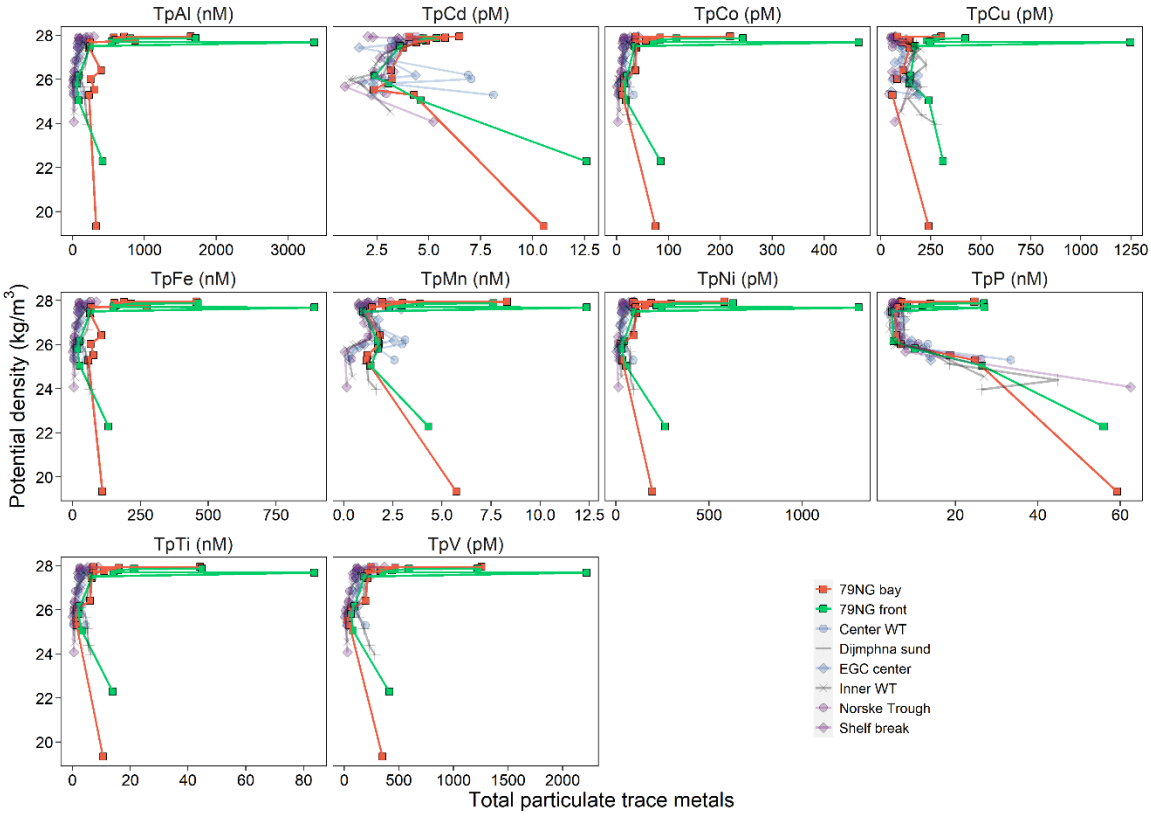

Fig. S4 Distribution profiles of total particulate (Tp) Cd, Co, Cu, Fe, Mn, Ni, Al, Ti, V, and P against potential density on the NE Greenland shelf.

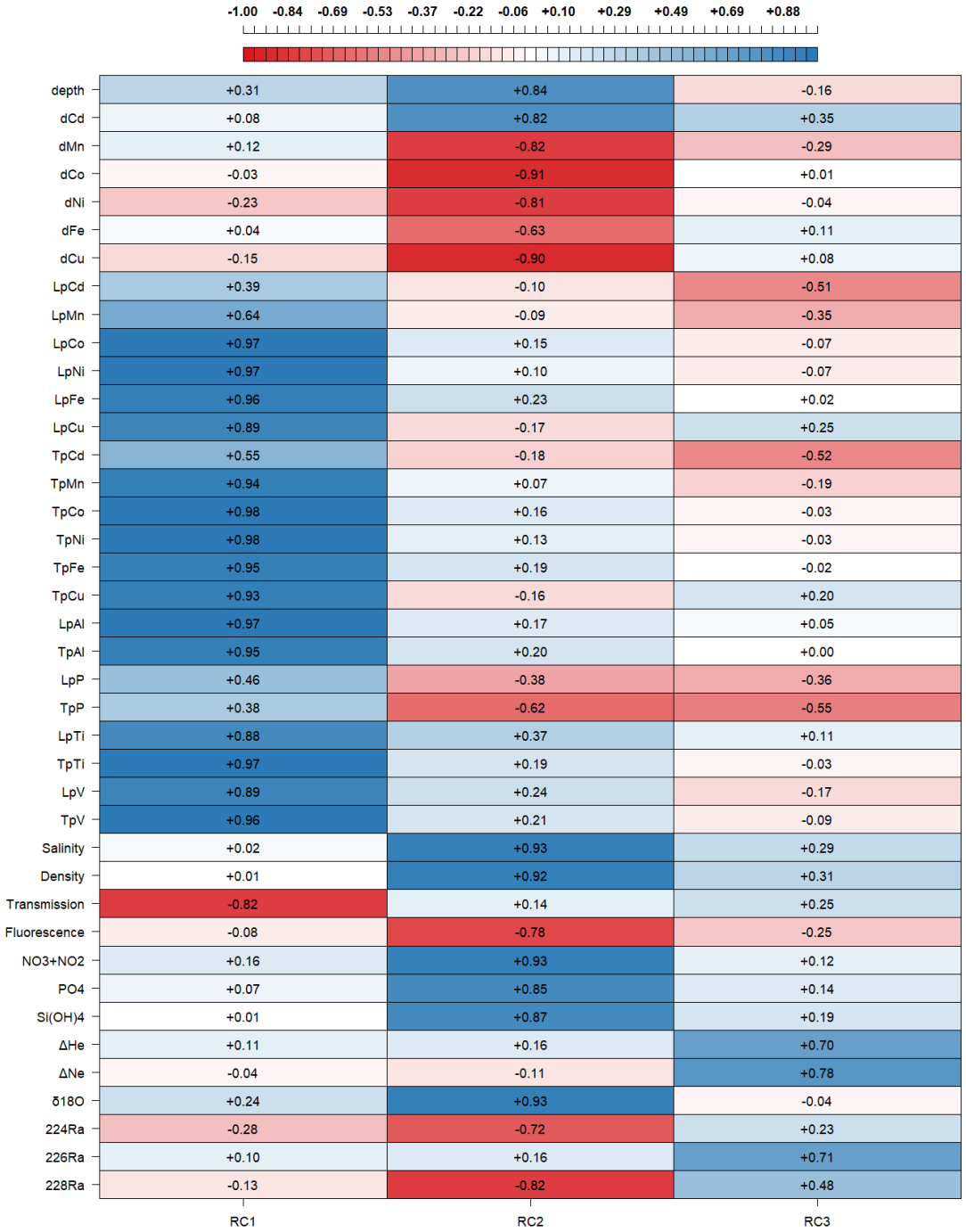

Fig. S5 Principal component analysis on the trace elements and physico-chemical parameters of the water columns collected during the GEOTRACES cruise GN05. The data are merged from ultraclean CTD (ucCTD) stations (dissolved and particulate trace elements, macronutrients, salinity, density, transmission, and fluorescence) and large volume CTD (lvCTD) stations ($\delta^{18}O$, noble gases, radium isotopes (^{224}Ra, ^{226}Ra, and ^{228}Ra)) as per Supplementary Methods. Helium excess (ΔHe) and neon excess (ΔNe) were calculated as per Supplementary Methods.

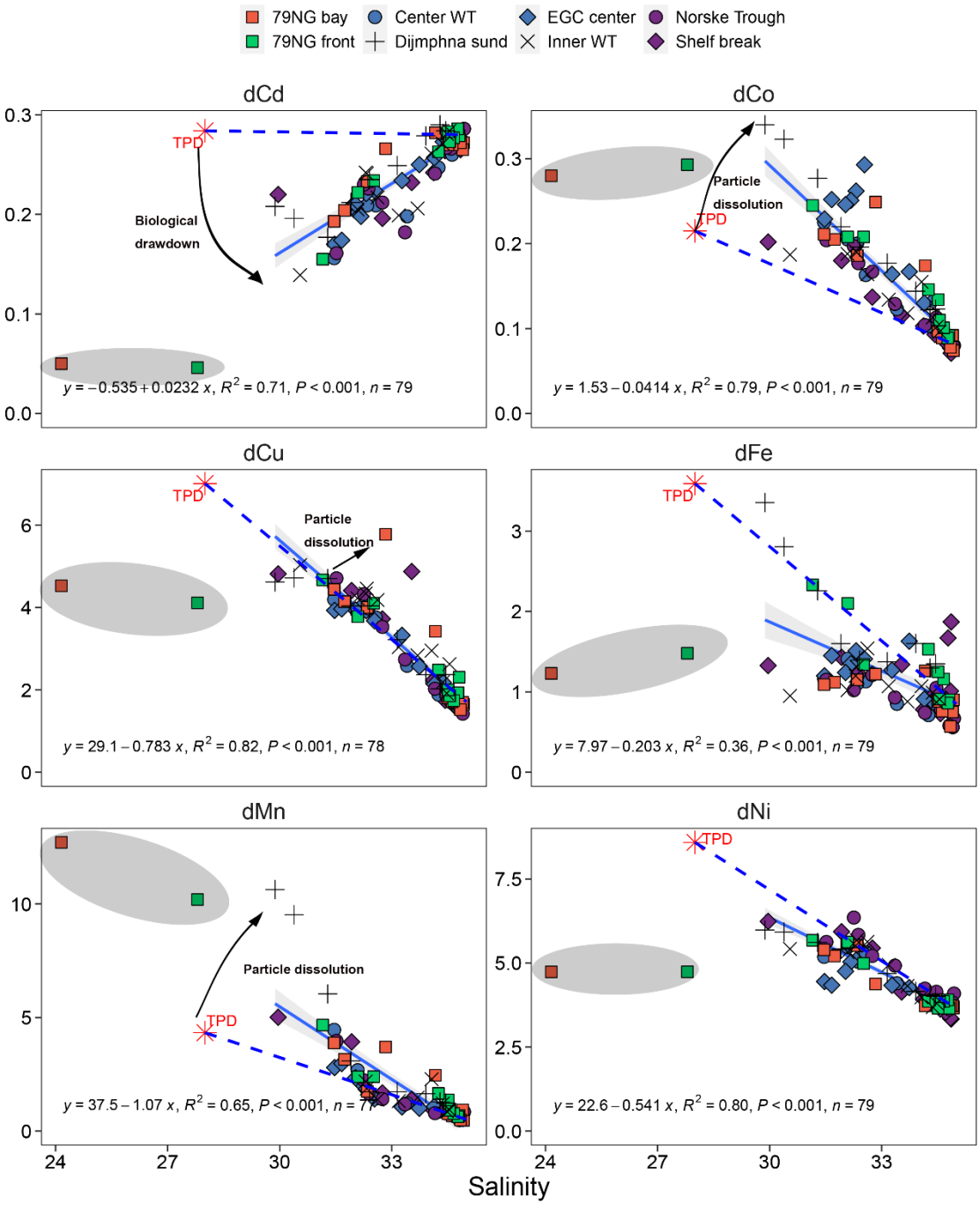

Fig. S6 Correlations between dissolved trace metals (dTMs, all in nM) and salinity on the NE Greenland shelf. Data with salinity < 28 (the two near surface samples from 79NG front and 79NG bay, encircled in grey ellipses) were excluded from linear regression models (blue solid lines). The dTM concentrations of transpolar drift (TPD) with meteoric water percentage of 20% (the highest meteoric water contribution observed in TPD) are also shown for comparison (Charette et al., 2020). The blue dashed lines illustrate the conservative mixing between AIW and Arctic waters (represented by TPD with 20% meteoric water). *n* indicates the number of samples in the linear regression models.

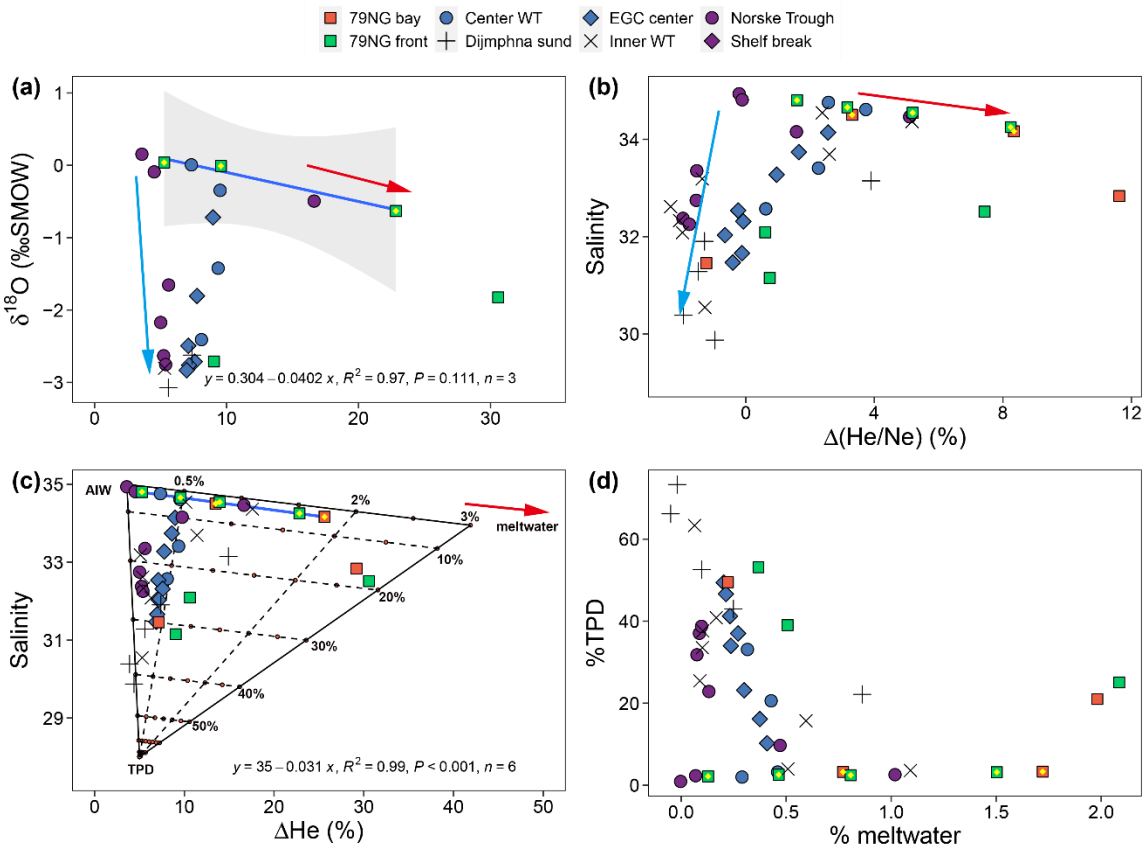

Fig. S7 Variations of $\delta^{18}O$ with (a) helium excess (ΔHe), and changes of salinity with (b) Δ(He/Ne) and (c) ΔHe in the water columns on the NE Greenland shelf. (d) Estimated contributions of submarine meltwater and Arctic waters (represented by transpolar drift (TPD) with 20% meteoric water) on the NE Greenland shelf using the following endmembers: Atlantic Intermediate Water (AIW), salinity = 35, ΔHe = 3.6%; TPD, salinity = 28 (20% meteoric water), ΔHe = 5.0%; and meltwater, salinity = 0, ΔHe = 1280% (e.g., Beaird et al., 2015; Loose & Jenkins, 2014). Blue arrows indicate the mixing between AIW and Arctic waters. Red arrows suggest the input of basal meltwater from the 79NG cavity. Linear regression models (blue lines) only apply to the 79NG samples with depths of > 100 m (highlighted with yellow diamonds) to illustrate the mixing between AIW and submarine meltwater. *n* indicates the number of samples in the linear regression models.

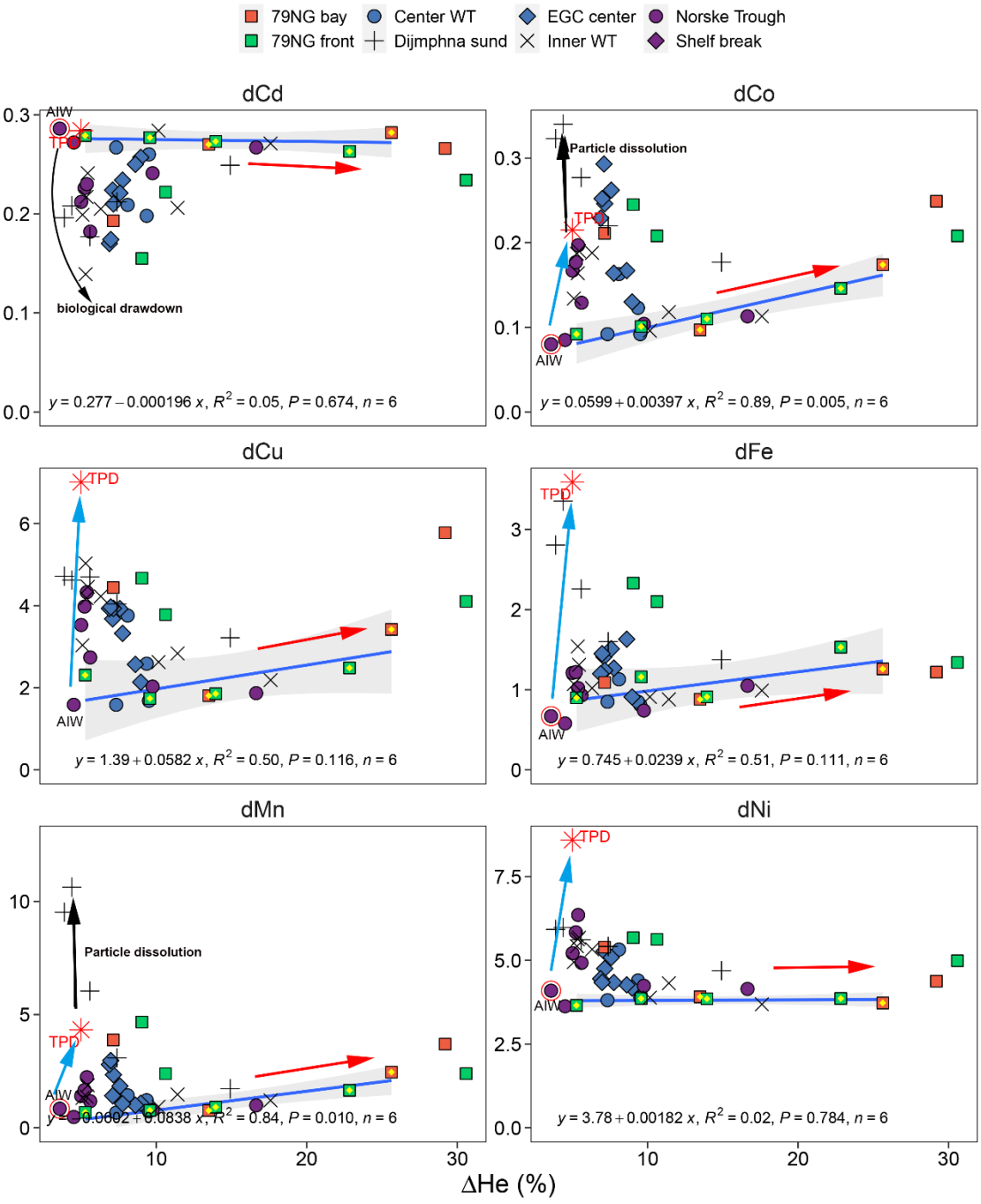

Fig. S8 Correlations between dissolved trace metals (dTMs) and helium excess (ΔHe) on NE Greenland shelf. Blue arrows indicate the mixing between AIW and Arctic waters (shown in red asterisks, represented by transpolar drift (TPD) with 20% meteoric water) (Charette et al., 2020), while red arrows illustrate the influence of submarine meltwater. Blue lines with grey shadows illustrate fitted linear regression models with 95% confidence levels. The red encircled sample represents the inflowing AIW. Linear regression models only apply to the 79NG samples with depths of > 100 m (highlighted with yellow diamonds) by excluding

the samples with significant influence of Arctic waters. *n* indicates the number of samples in the linear regression models.

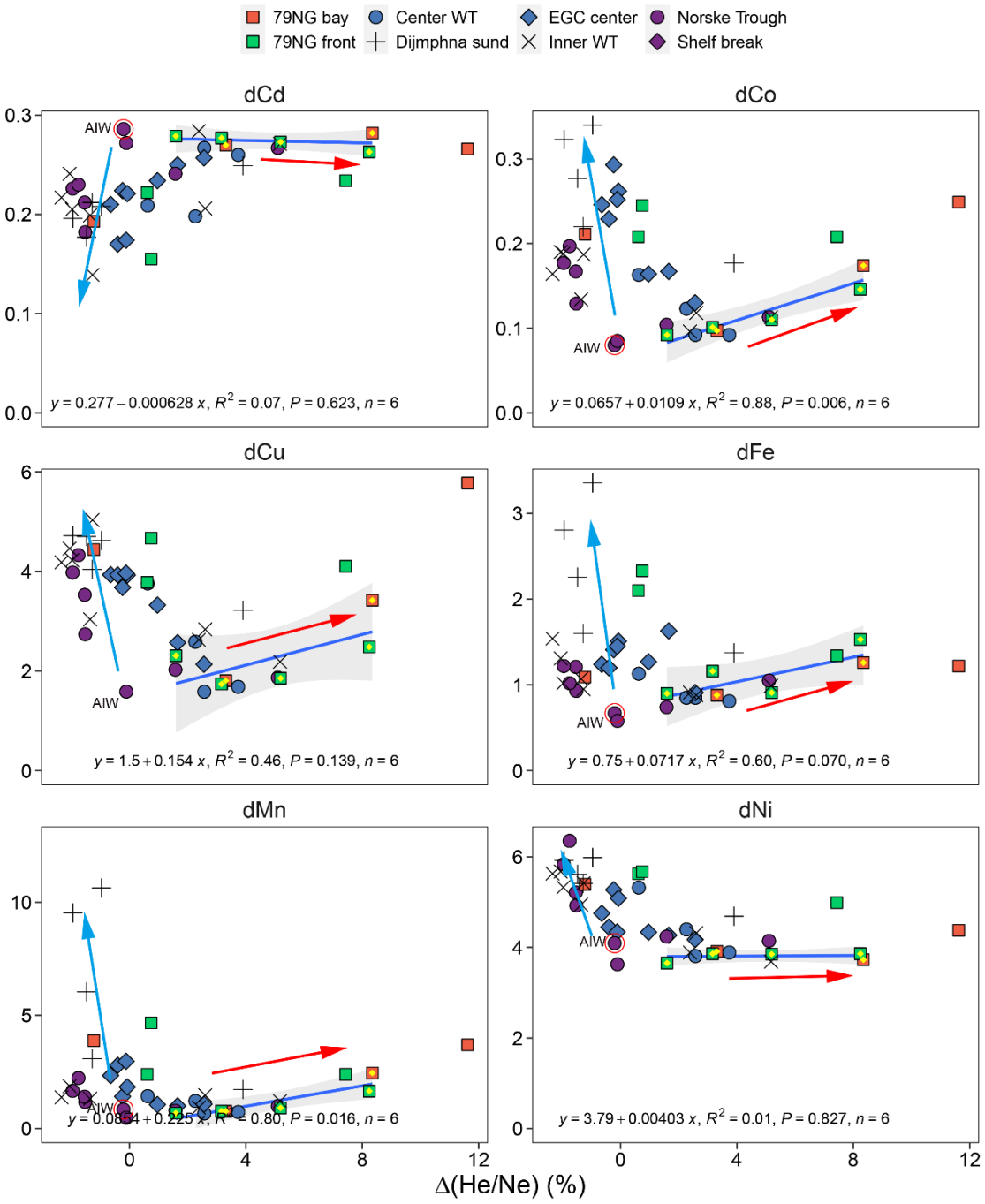

Fig. S9 Correlations between dissolved trace metals (dTMs) and Δ(He/Ne) on NE Greenland shelf. Blue arrows indicate the mixing between AIW and Arctic waters, while red arrows illustrate the influence of submarine meltwater (through sediment-water exchange). Blue lines with grey shadows illustrate fitted linear regression models with 95% confidence levels. The red encircled sample represents the inflowing AIW. Linear regression models only apply to the 79NG samples with depths of > 100 m (highlighted with yellow

diamonds) by excluding the samples with significant influence of Arctic waters. *n* indicates the number of samples in the linear regression models.

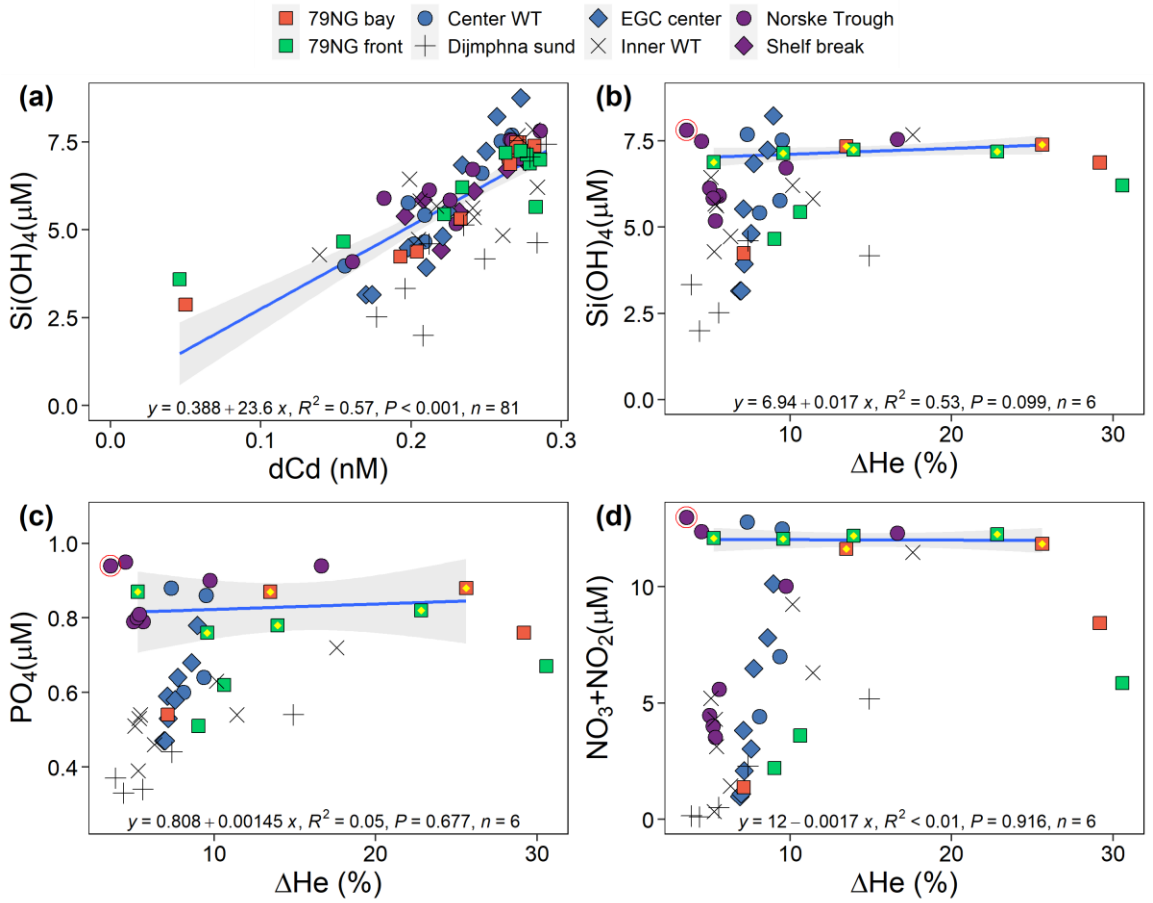

Fig. S10 Correlations of $Si(OH)_4$ – dCd and those between macronutrients and helium excess (ΔHe) on the NE Greenland shelf. The red encircled sample represents the inflowing Atlantic Intermediate Water (AIW). Linear regression models (blue lines with 95% confidence levels) in Fig. (b, c, and d) only apply to the 79NG samples with depths of > 100 m (highlighted with yellow diamonds). *n* indicates the number of samples in the linear regression models.

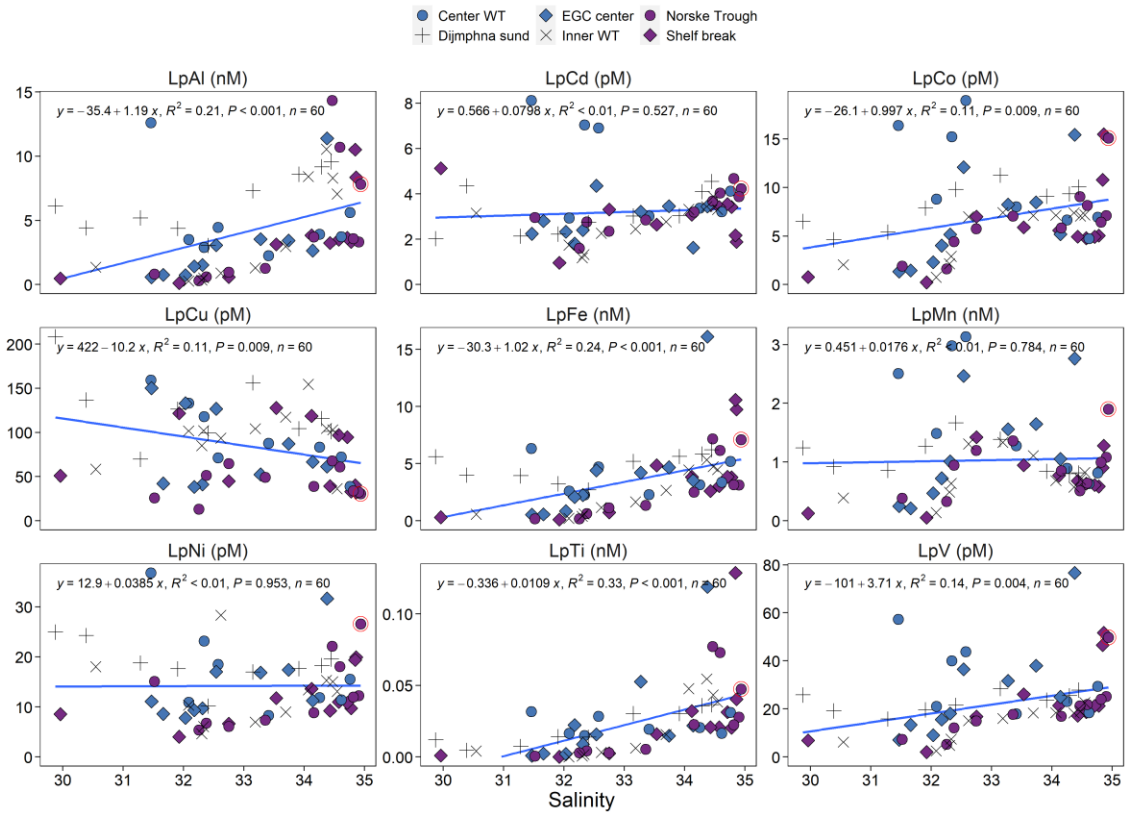

Fig. S11 Variations of LpTMs (Al, Cd, Co, Ni, Cu, Fe, Mn, Ti, and V) across the salinity gradients on the NE Greenland shelf. The sample in red circle from the Norske Trough represents the inflowing Atlantic Intermediate Water (AIW). Linear regression models (blue lines) are applied to all samples. *n* indicates the number of samples in the linear regression models.

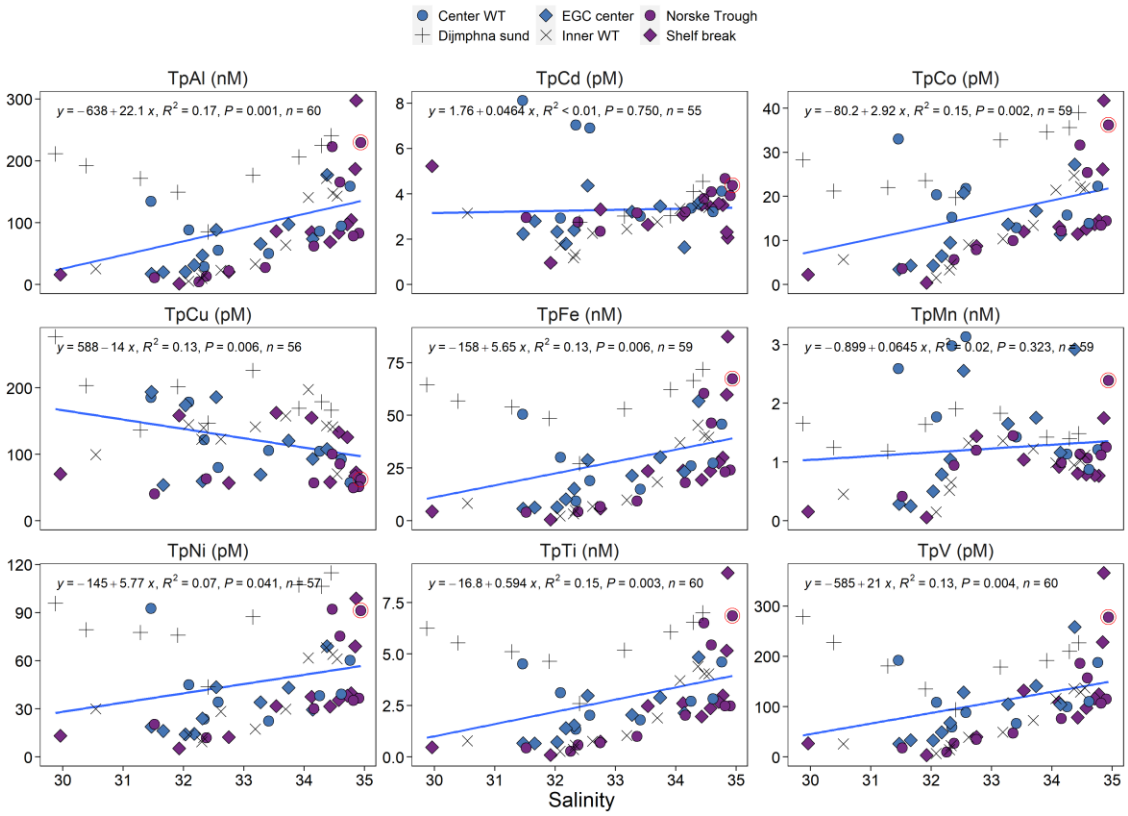

Fig. S12 Variations of TpTMs (Al, Cd, Co, Ni, Cu, Fe, Mn, Ti, and V) across the salinity gradients on the NE Greenland shelf. The sample in red circle from the Norske Trough represents the inflowing Atlantic Intermediate Water (AIW). Linear regression models (blue lines) are applied to all samples. *n* indicates the number of samples in the linear regression models.

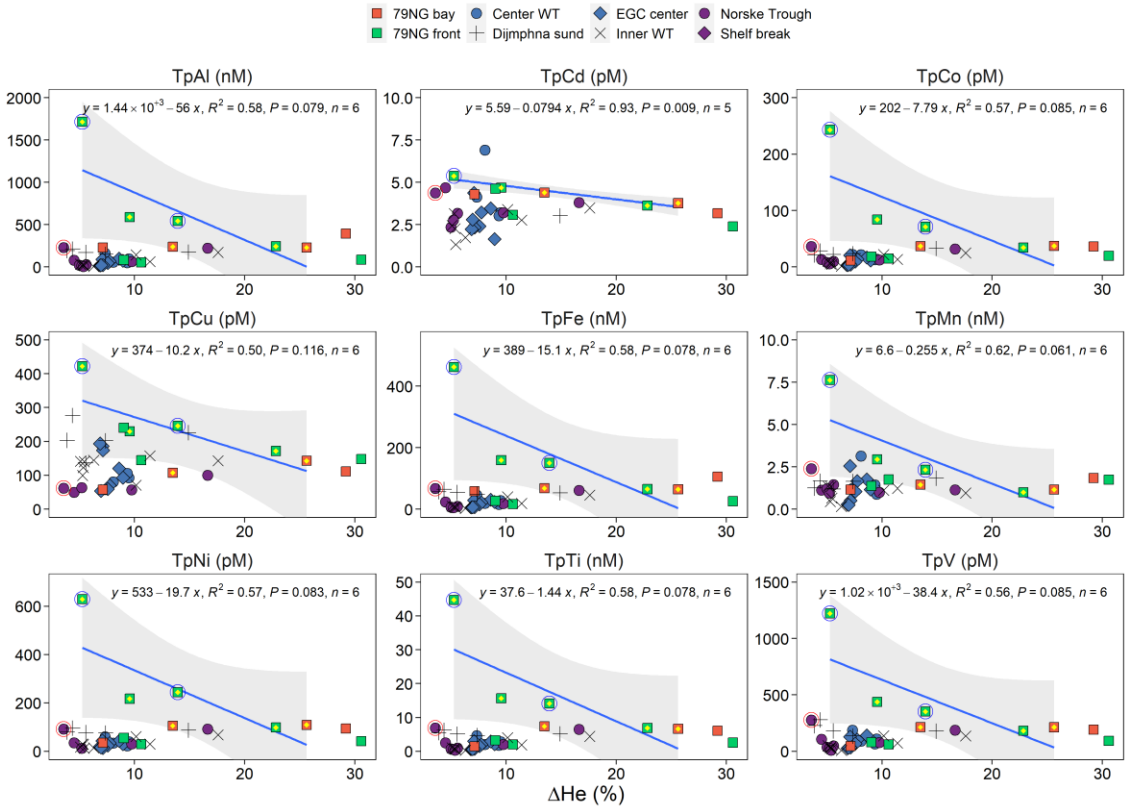

Fig. S13 Variations of total particulate trace metals (TpTMs) with helium excess (ΔHe) on the NE Greenland shelf. The red encircled sample represents the inflowing AIW, while the blue encircled samples indicate high turbidity. Linear regression models (blue lines with 95% confidence levels) only apply to the 79NG samples with depths > 100 m (highlighted with yellow diamonds) to demonstrate the influence of mAIW exiting from the 79NG cavity. *n* indicates the number of samples in the linear regression models.

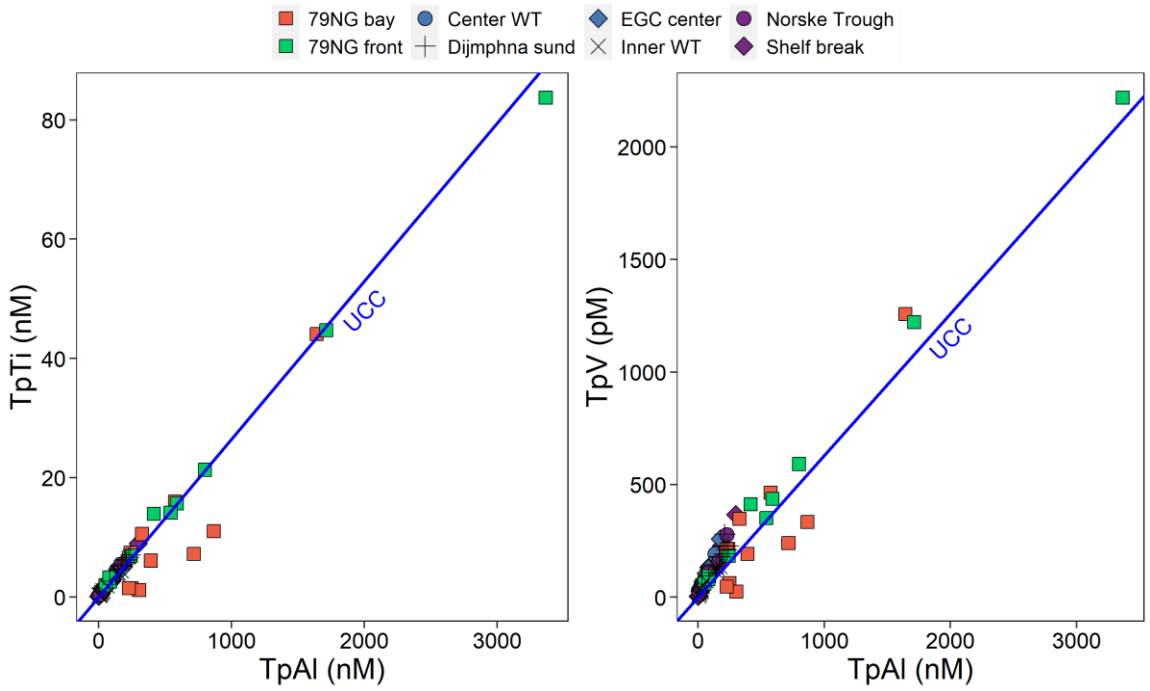

Fig. S14 Correlations between TpTi, TpV and TpAl in the water columns on the NE Greenland shelf. The blue lines illustrate the upper continental crust (UCC) values (Rudnick & Gao, 2003).

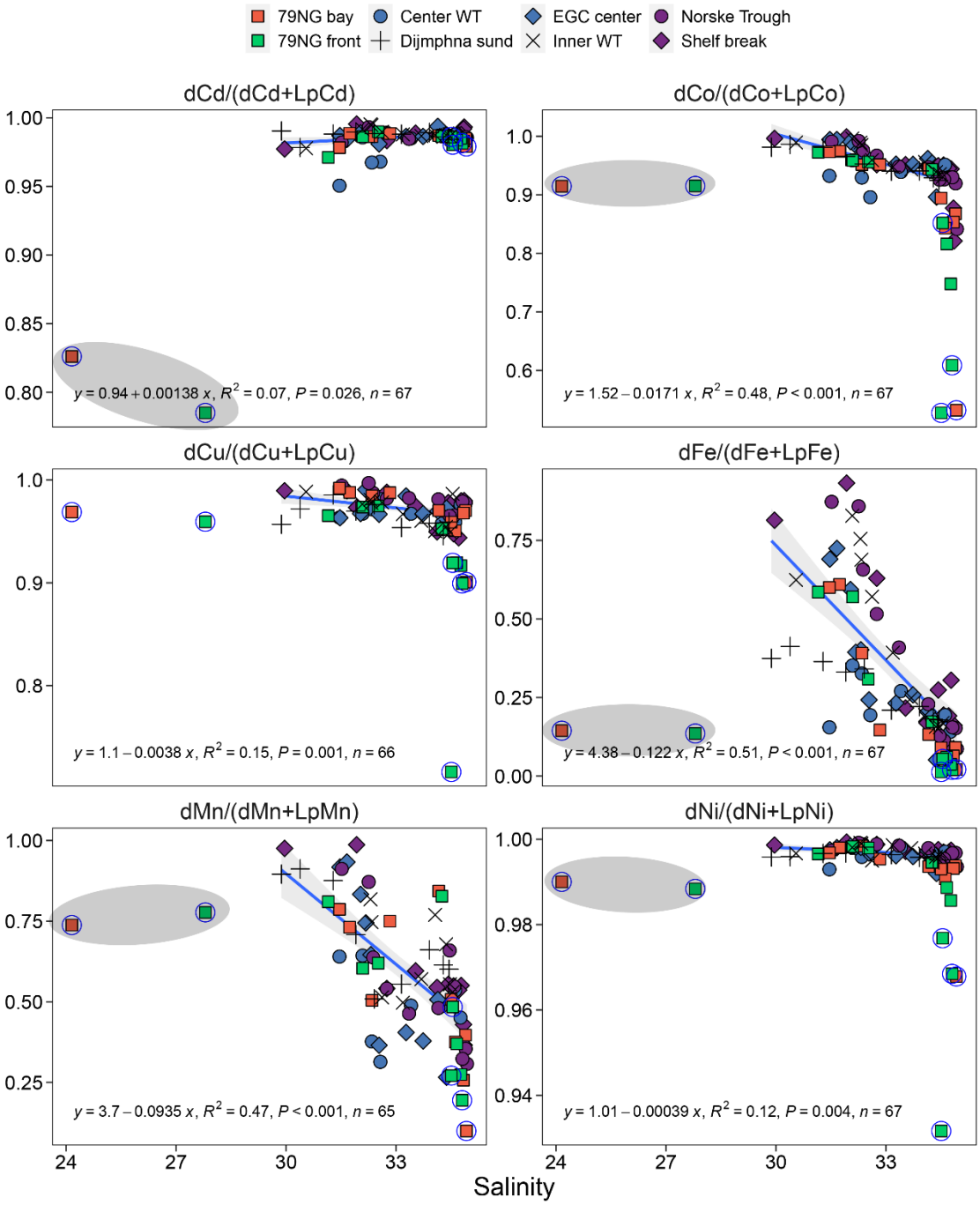

Fig. S15 Variations of dTM/(dTM+LpTM) ratios across the salinity gradients on the NE Greenland shelf. The turbid samples (light transmission < 4.4) and two surface samples at 79NG stations (with a salinity of < 28, encircled in grey ellipses), denoted in blue circles, are excluded from linear regression models (blue lines with 95% confidence levels). *n* indicates the number of samples in the linear regression models.

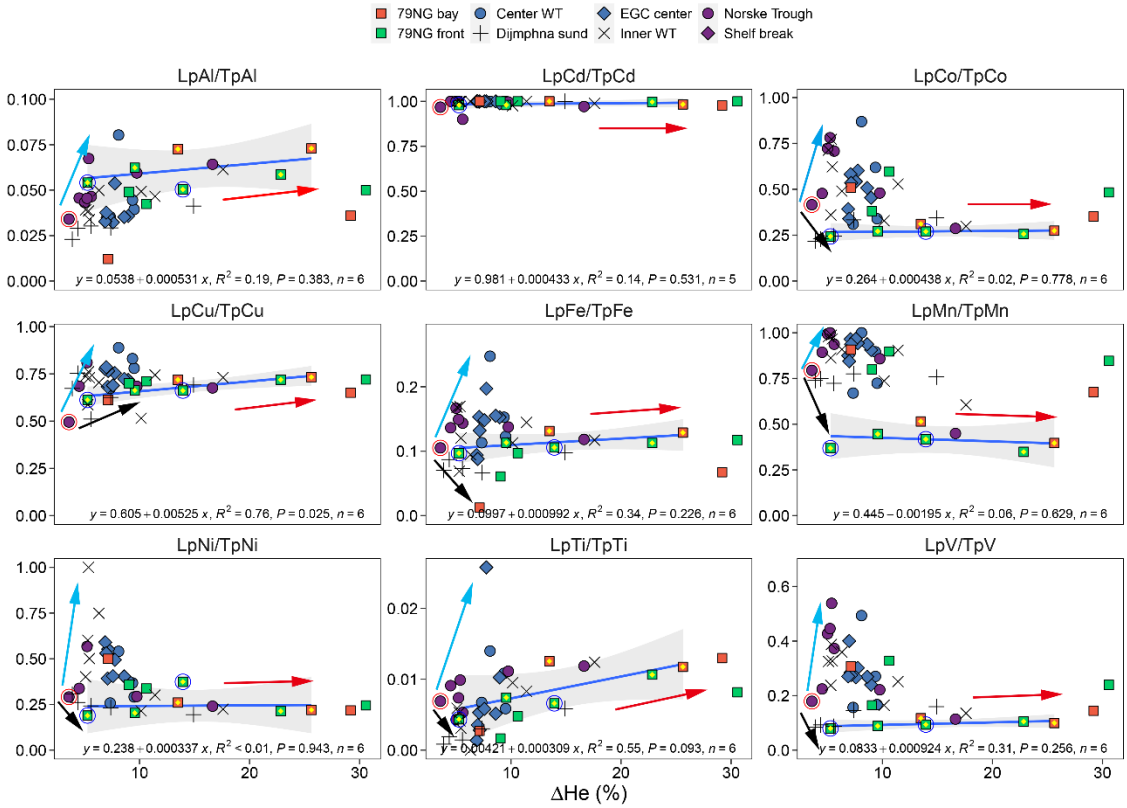

Fig. S16 Changes of trace metal labile fractions (LpTM/TpTM) with helium excess (ΔHe) in the water columns on the NE Greenland shelf. Blue arrows indicate the involvement of Arctic waters, while red arrows suggest the addition of submarine meltwater. Black arrows demonstrate the potential influence of sediment particles. The red encircled sample represents the inflowing Atlantic Intermediate Water (AIW), while the blue encircled samples indicate high turbidity. Linear regression models (blue lines with 95% confidence levels) only apply to the 79NG samples with depths > 100 m (highlighted with yellow diamonds). *n* indicates the number of samples in the linear regression models.

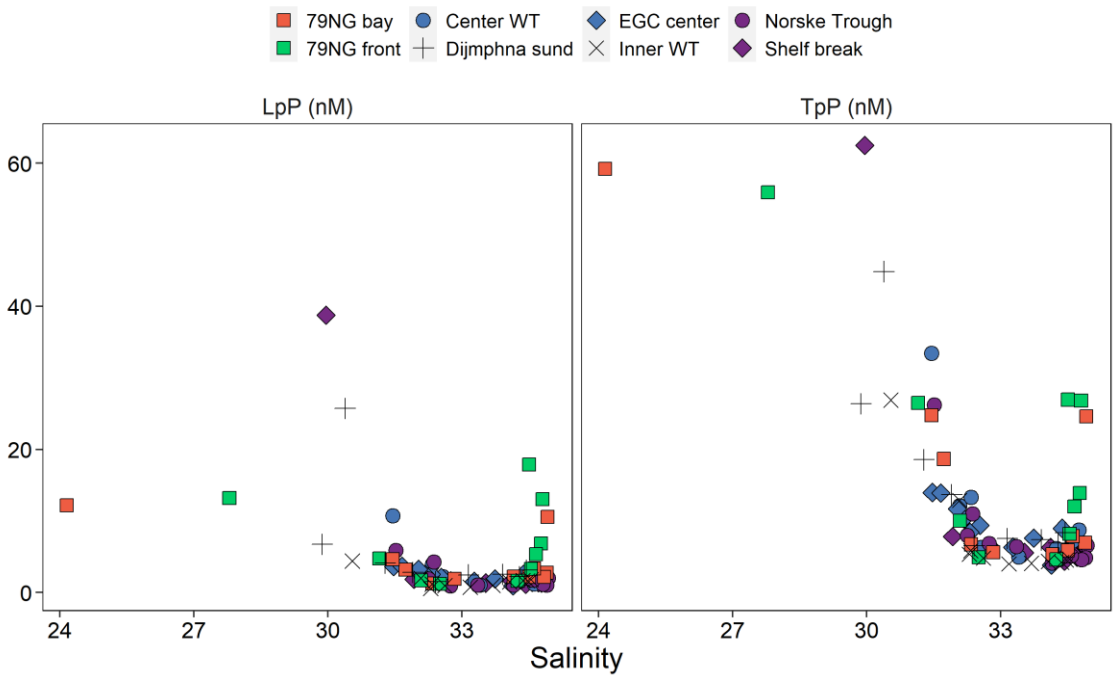

Fig. S17 Variations of labile particulate P (LpP) and total particulate P (TpP) across the salinity gradient on the NE Greenland shelf.

Table S2 Comparison of dissolved trace metal (dTM) concentrations (nM) of apparent Atlantic Intermediate Water (AIW) and freshwater endmembers. The endmember dTM contents of this study are shown in estimated values with 95% confidence levels. The endmember dTM values proposed by Charette et al. (2020) and Krisch et al. (2022) are derived from their linear regression models. *Inclusive of NE Greenland shelf data.

Water masses	**References**	**dFe**	**dMn**	**dCo**	**dNi**	**dCu**	**dCd**
AIW (salinity of 35)	This study	0.85 ± 0.12	0.51 ± 0.21	0.08 ± 0.01	3.65 ± 0.13	1.71 ± 0.19	0.28 ± 0.05
AIW	Krisch et al. (2022)	0.61 ± 0.08	0.64 ± 0.12	0.087 ± 0.008	3.79 ± 0.15	1.60 ± 0.11	not calculated
Freshwater endmember for the NE Greenland shelf	This study	7.97 ± 2.06	25.8 ± 3.7	1.54 ± 0.16	22.6 ± 2.0	29.2 ± 2.7	<0
Freshwater endmember for the Fram Strait*	Krisch et al. (2022)	4.3 (R^2=0.21)	15.5 (R^2=0.45)	0.97 (R^2=0.73)	17.2 (R^2=0.78)	21.2 (R^2=0.88)	not calculated
Freshwater endmember for Southwest and west Greenland shelf	van Genuchten et al. (2022); Krause et al. (2021)	26.0 (R^2=0.06)	84.9 (R^2=0.29)	2.66 (R^2 = 0.10)	10.8 (R^2 = 0.04)	6.61 (R^2=0.01)	not calculated
Arctic freshwater	Charette et al. (2020)	19.3 (R^2=0.67)	16.4 (R^2=0.41)	0.85 (R^2=0.54)	30.6 (R^2=0.91)	30.1 (R^2=0.96)	1.22 (R^2=0.66)
Submarine meltwater from the 79NG cavity	This study	31.4 ± 41.2	107 ± 63.7	5.15 ± 2.49	6.12 ± 21.9	75.9 ± 102	0.03 ± 1.52
Ob river	Dai and Martin, (1995)	429.7 – 654.2	not analyzed	not analyzed	21.0 – 23.7	29.1 – 38.0	5.4 – 7.5
Yenisey river		251.0 – 317.1	not analyzed	not analyzed	8.8 – 9.4	21.5 – 29.5	10.7 – 16.4
Lena river	(Guieu et al., 1996)	642 ± 208	not analyzed	not analyzed	4.4 ± 0.1	13.8 ± 1.6	0.054 ± 0.047

Supplementary References

Al-Hashem, A. A., Beck, A. J., Krisch, S., Menzel Barraqueta, J.-L., Steffens, T., & Achterberg, E. P. (2022). Particulate Trace Metal Sources, Cycling, and Distributions on the Southwest African Shelf. *Global Biogeochemical Cycles*, *36*(11), e2022GB007453. https://doi.org/10.1029/2022GB007453

Beaird, N., Straneo, F., & Jenkins, W. (2015). Spreading of Greenland meltwaters in the ocean revealed by noble gases. *Geophysical Research Letters*, *42*(18), 7705–7713. https://doi.org/10.1002/2015GL065003

Berger, C. J. M., Lippiatt, S. M., Lawrence, M. G., & Bruland, K. W. (2008). Application of a chemical leach technique for estimating labile particulate aluminum, iron, and manganese in the Columbia River plume and coastal waters off Oregon and Washington. *Journal of Geophysical Research: Oceans*, *113*(C2), C00B01. https://doi.org/10.1029/2007JC004703

Charette, M. A., Kipp, L. E., Jensen, L. T., Dabrowski, J. S., Whitmore, L. M., Fitzsimmons, J. N., et al. (2020). The Transpolar Drift as a Source of Riverine and Shelf-Derived Trace Elements to the Central Arctic Ocean. *Journal of Geophysical Research: Oceans*, *125*(5), e2019JC015920. https://doi.org/10.1029/2019JC015920

Cullen, J. T., & Sherrell, R. M. (1999). Techniques for determination of trace metals in small samples of size-fractionated particulate matter: phytoplankton metals off central California. *Marine Chemistry*, *67*(3), 233–247. https://doi.org/10.1016/S0304-4203(99)00060-2

Cullen, J. T., Field, M. P., & Sherrell, R. M. (2001). Determination of trace elements in filtered suspended marine particulate material by sector field HR-ICP-MS. *Journal of Analytical Atomic Spectrometry*, *16*(11), 1307–1312. https://doi.org/10.1039/B104398F

Cutter, G., Casciotti, K., Croot, P., Geibert, W., Heimbürger, L.-E., Lohan, M., et al. (2017). Sampling and Sample-handling Protocols for GEOTRACES Cruises. Version 3, August 2017. *GEOTRACES Standards and Intercalibration Committee*.

Dai, M.-H., & Martin, J.-M. (1995). First data on trace metal level and behaviour in two major Arctic river-estuarine systems (Ob and Yenisey) and in the adjacent Kara Sea, Russia. *Earth and Planetary Science Letters*, *131*(3), 127–141. https://doi.org/10.1016/0012-821X(95)00021-4

van Genuchten, C. M., Hopwood, M. J., Liu, T., Krause, J., Achterberg, E. P., Rosing, M. T., & Meire, L. (2022). Solid-phase Mn speciation in suspended particles along meltwater-influenced fjords of West Greenland. *Geochimica et Cosmochimica Acta*, *326*, 180–198. https://doi.org/10.1016/j.gca.2022.04.003

Grasshoff, K., Kremlingl, K., & Ehrhardt, M. (1999). *Methods of Seawater Analysis* (3rd ed.). Weinheim: WILEY-VCH Verlag GmbH. https://doi.org/10.1002/9783527613984

Guieu, C., Huang, W. W., Martin, J.-M., & Yong, Y. Y. (1996). Outflow of trace metals into the Laptev Sea by the Lena River. *Marine Chemistry*, *53*(3), 255–267. https://doi.org/10.1016/0304-4203(95)00093-3

Huhn, O., Rhein, M., Bulsiewicz, K., & Sültenfuß, J. (2021). Noble gas (He, Ne isotopes) and transient tracer (CFC-11 and CFC-12) measurements from POLARSTERN cruise PS100 (northeast Greenland, 2016) [Data set]. PANGAEA. https://doi.org/10.1594/PANGAEA.931336

Huhn, O., Rhein, M., Kanzow, T., Schaffer, J., & Sültenfuß, J. (2021). Submarine Meltwater From Nioghalvfjerdsbræ (79 North Glacier), Northeast Greenland. *Journal of Geophysical Research: Oceans*, *126*(7), e2021JC017224. https://doi.org/10.1029/2021JC017224

Jochum, K. P., Nohl, U., Herwig, K., Lammel, E., Stoll, B., & Hofmann, A. W. (2005). GeoReM: A New Geochemical Database for Reference Materials and Isotopic Standards. *Geostandards and Geoanalytical Research*, *29*(3), 333–338. https://doi.org/10.1111/j.1751-908X.2005.tb00904.x

Kanzow, T., von Appen, W.-J., Schaffer, J., Köhn, E., Tsubouchi, T., Wilson, N., & Wisotzki, A. (2017). Physical oceanography measured on water bottle samples from CTD/Large volume Watersampler-system during POLARSTERN cruise PS100 (ARK-XXX/2) [Data set]. *Alfred Wegener Institute, Helmholtz Centre for Polar and Marine Research, Bremerhaven*. PANGAEA. https://doi.org/10.1594/PANGAEA.871028

Kanzow, T., von Appen, W.-J., Schaffer, J., Köhn, E., Tsubouchi, T., Wilson, N., Lodeiro, P. F., et al. (2017). Physical oceanography measured with ultra clean CTD/Watersampler-system during POLARSTERN cruise PS100 (ARK-XXX/2) [Data set]. *Alfred Wegener Institute, Helmholtz*

Centre for Polar and Marine Research, Bremerhaven. PANGAEA. https://doi.org/10.1594/PANGAEA.871030

Krause, J., Hopwood, M. J., Höfer, J., Krisch, S., Achterberg, E. P., Alarcón, E., et al. (2021). Trace Element (Fe, Co, Ni and Cu) Dynamics Across the Salinity Gradient in Arctic and Antarctic Glacier Fjords. *Frontiers in Earth Science*, *9*, 878. https://doi.org/10.3389/feart.2021.725279

Krisch, S., Hopwood, M. J., Schaffer, J., Al-Hashem, A., Höfer, J., Rutgers van der Loeff, M. M., et al. (2021). The 79°N Glacier cavity modulates subglacial iron export to the NE Greenland Shelf. *Nature Communications*, *12*(1), 3030. https://doi.org/10.1038/s41467-021-23093-0

Krisch, S., Hopwood, M. J., Roig, S., Gerringa, L. J. A., Middag, R., Rutgers van der Loeff, M. M., et al. (2022). Arctic – Atlantic exchange of the dissolved micronutrients Iron, Manganese, Cobalt, Nickel, Copper and Zinc with a focus on Fram Strait. *Global Biogeochemical Cycles*, *36*(5), e2021GB007191. https://doi.org/10.1029/2021GB007191

Loose, B., & Jenkins, W. J. (2014). The five stable noble gases are sensitive unambiguous tracers of glacial meltwater. *Geophysical Research Letters*, *41*(8), 2835–2841. https://doi.org/10.1002/2013GL058804

Meyer, H., Schönicke, L., Wand, U., Hubberten, H. W., & Friedrichsen, H. (2000). Isotope studies of hydrogen and oxygen in ground ice - Experiences with the equilibration technique. *Isotopes in Environmental and Health Studies*, *36*(2), 133–149. https://doi.org/10.1080/10256010008032939

Meyer, Hanno, Schaffer, J., Rabe, B., & Rutgers van der Loeff, M. M. (2021). Oxygen and hydrogen isotopes in water samples collected during Polarstern cruise PS100 in 2016 [Data set]. PANGAEA. https://doi.org/10.1594/PANGAEA.927429

Rapp, I., Schlosser, C., Rusiecka, D., Gledhill, M., & Achterberg, E. P. (2017). Automated preconcentration of Fe, Zn, Cu, Ni, Cd, Pb, Co, and Mn in seawater with analysis using high-resolution sector field inductively-coupled plasma mass spectrometry. *Analytica Chimica Acta*, *976*, 1–13. https://doi.org/10.1016/j.aca.2017.05.008

Rudnick, R. L., & Gao, S. (2003). Composition of the continental crust. In *The Crust*. Oxford: Elsevier-Pergamon.

Rutgers van der Loeff, M. M., Kipp, L., Charette, M. A., Moore, W. S., Black, E., Stimac, I., et al. (2018). Radium Isotopes Across the Arctic Ocean Show Time Scales of Water Mass Ventilation and Increasing Shelf Inputs. *Journal of Geophysical Research: Oceans*, *123*(7), 4853–4873. https://doi.org/10.1029/2018JC013888

Sültenfuß, J., Roether, W., & Rhein, M. (2009). The Bremen mass spectrometric facility for the measurement of helium isotopes, neon, and tritium in water. *Isotopes in Environmental and Health Studies*, *45*(2), 83–95.

Weiss, R. F. (1971). Solubility of helium and neon in water and seawater. *Journal of Chemical & Engineering Data*, *16*(2), 235–241.